A Standardized Mechanism to Validate Crash Models for Ductile Plastics

Megan Lobdell[1], Brian Croop[1], Hubert Lobo[1]
[1]*DatapointLabs, Ithaca, NY*

Abstract

Quantifying simulation accuracy before running crash simulations could be a helpful confidence building measure. This study continues our development of a mechanism to validate material models for plastics used in modeling high-speed impact. Focusing on models for isotropic materials that include options for rate dependency and failure, we explore other models commonly used for ductile plastics including MAT089 and MAT187.

Introduction

Validating simulation accuracy prior to commencing design of actual parts and assemblies can bring confidence and valuable insights to the virtual product development process. Simulations often require a number of settings and data transformations, the correct combination of which can lead to a quality result. The determination of the right combination is a vital step early in the design process. Validation with standardized parts which contain geometric features that probe simulation accuracy can be a useful tool to increase the confidence in simulation and reduce the likelihood of prototype failure.

Material modeling can be a key contributor to the variability of a simulation. This is particularly true when the material models are complex, and there is more than one way to transform incoming material data into the parameters required for simulation. In previous work [1], we used a high-speed dart impact experiment to validate a simulation for two ductile plastics, an ABS and a polypropylene, using a MAT_024 material model. While the biaxial mode of deformation is believed to dominate, the experiment contains complex uniaxial, biaxial, and shear modes with eventual failure as the dart pierces through the material. It is a considered to be a reliable experiment for validation since it has well defined boundary conditions and loading conditions. For both materials, the simulation was seen to correlate well with the experiment up to peak force where an abrupt failure occurs. In the case of the polypropylene, the material exhibited the brittle failure predicted by the simulation, resulting in acceptable correlation. For the ABS, the simulation was unable to predict the softening behavior seen in the experiment (Figure 1). We further noted that an arbitrary failure strain, which was greater than the measured value in tension, was used in order obtain good correlation. The corresponding plasticity load curves also had to be extrapolated beyond the fail strain for this purpose.

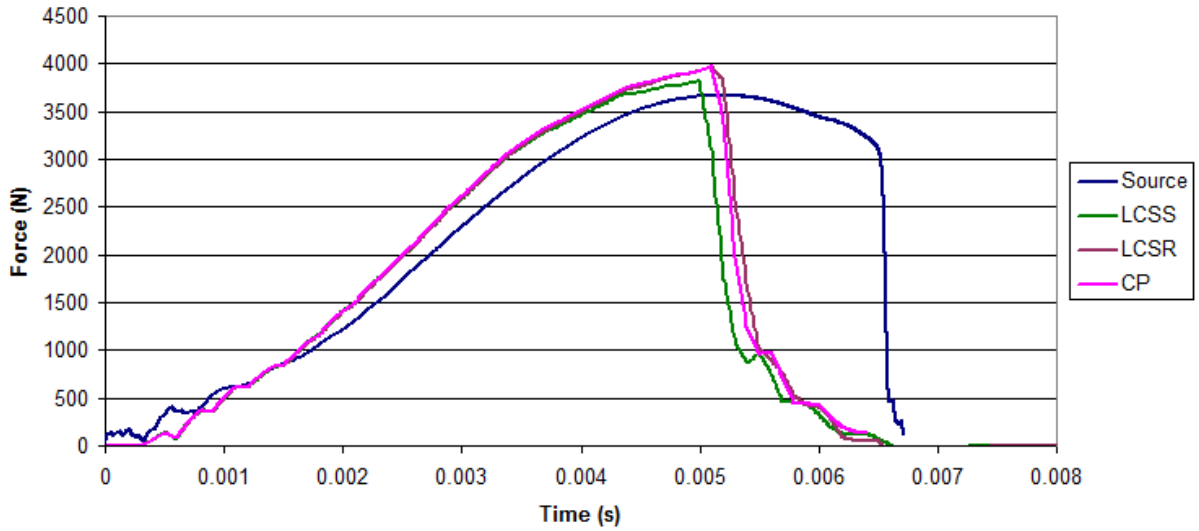

Figure 1: Final results of falling dart (open loop) validation of MAT_024 for ABS.

Where MAT_024 was originally designed for simulating metals, other material models such as MAT_089 and MAT_187 exist which have been developed for polymers. In an attempt to overcome some of the assumptions needed in the previous work [1], we examined different configurations of these models to see what improvements to simulation accuracy could be realized.

Procedure

The material parameters for MAT_089 can be generated from the same data as are needed for MAT_024 [2]. An important difference is that the model accepts true stress versus equivalent strain instead of plastic strain. A useful feature of MAT_089 is the ability to model the failure strain as a function of strain rate. This is important for plastics that exhibit rate-dependent failure, such as the polypropylene used in our study.

MAT_187 requires two or more additional quasi-static experiments to describe the other modes of deformation. The material model also requires the quasi-static tensile test to be processed with digital image correlation (DIC) techniques to produce a post-yield Poisson's ratio. The post-yield (plasticity) Poisson's ratio, shear stress, and compression stress curves are supplied to the model as functions of plastic strain. Finally, failure strains can be modeled as a function of stress triaxiality, and if desired, strain rate.

We performed quasi-static tensile tests with DIC to obtain stress v. strain in x, y, and z directions; combined loading compression (ASTM D6641) to obtain compressive stress-strain curves; and Iosipescu shear (ASTM D5379) experiments with DIC to obtain the shear properties. Details of the testing have been described previously [3]; the only improvement was the use of a combined loading compression fixture for the in-plane compressive tests. The experiments were run on the same Instron 8872 universal testing machine used for the original tensile tests [1]. As with our previous work, the goal of this study was to be able to use measured material properties as far as possible, thereby setting up a solid base for more complex simulations. The same template as that used for the previous MAT_024 simulations was used for all the current work,

where the material model tables and curves were the only varied option. Hourglass, element formulation, element size, and other options for the simulation were kept unchanged.

Results and Discussion

ABS Material Properties

The rate dependent properties of the ABS are shown in Figure 2. The measurements are not based on DIC and so, do not incorporate localized strain measurements. Aside from one strain rate, which we would note as an anomaly, failure strain is quite independent of strain rate. The modulus is also rate independent.

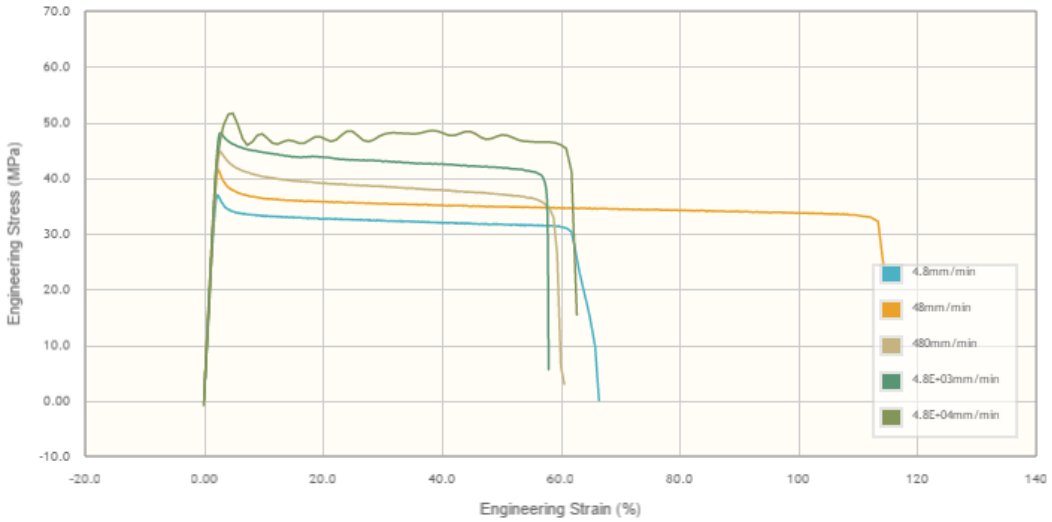

Figure 2: Rate-dependent tensile properties of ABS.

For the MAT_187 model, multi-mode data was obtained in addition to three-dimensional strain measurements to quantify the Poisson's ratio in the post-yield plasticity region. Attributing the lower modulus in compressive stress-strain to an anomaly, we modified the input curve for compressive data to use the same modulus as for the tensile data.

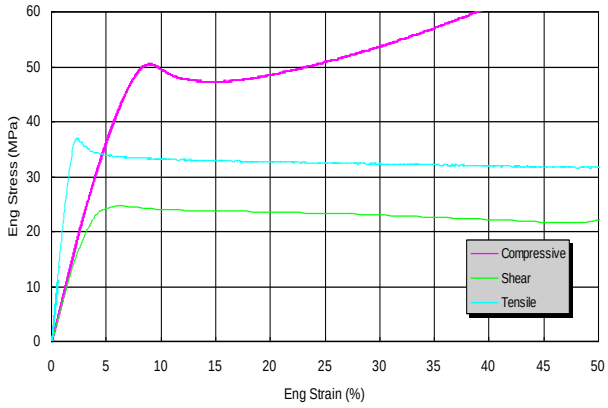

Figure 3: Stress-strain data in multiple modes for ABS.

Polypropylene Material Properties

The polypropylene showed significant rate dependency of failure strain with strain rate (Figure 4). Close examination of the initial region of the stress-strain curve indicates dependency of modulus with strain rate.

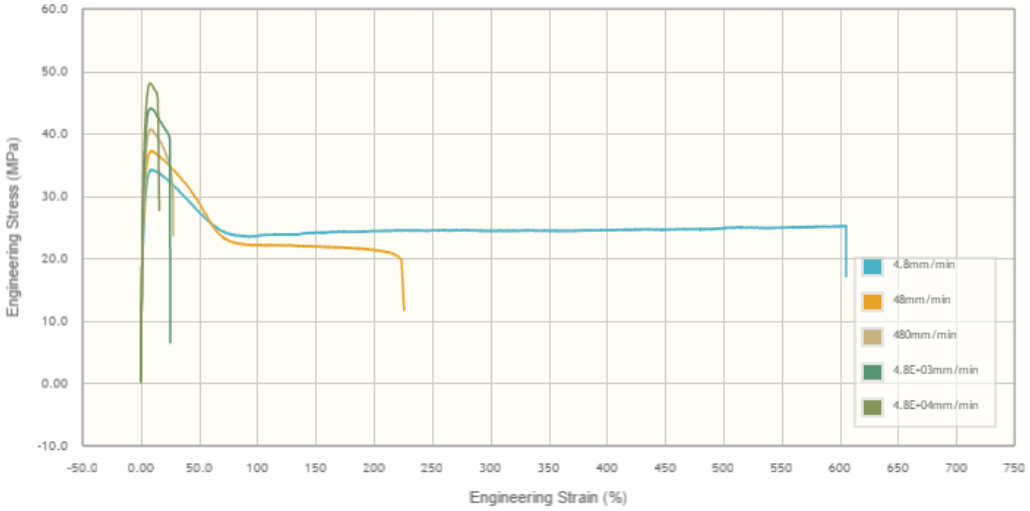

Figure 4: Rate dependent data for polypropylene.

For the MAT_187 model, multi-mode data was also obtained in addition to three-dimensional strain measurements to quantify the Poisson's ratio in the post-yield plasticity region.

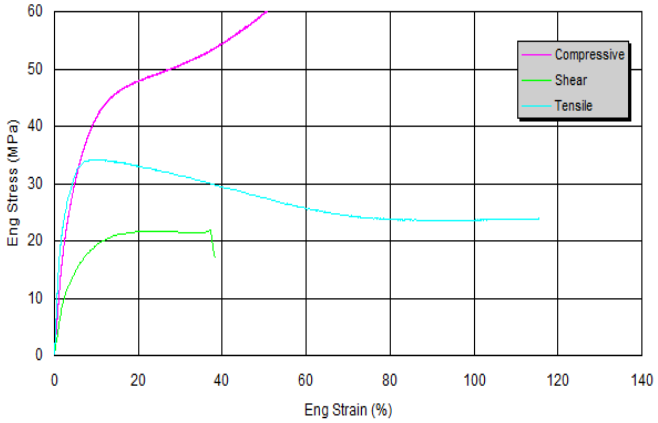

Figure 5: Multi-mode data for polypropylene--Stress v. Strain.

Dart Impact Simulation

The material model parameters, CP coefficients, LCSS table, or LCSR curves were calculated from the tensile tests at different strain rates using Matereality CAE Modeler for LS-DYNA Software. CP, LCSS, and LCSR are the three available rate dependency options for mat24 and mat89. As noted earlier, the simulation of the ABS material with a MAT_024 model and an arbitrary failure strain of 1.2 resulted in an abrupt failure, as seen in Figure 1. Extending the failure strain

beyond 1.2 shows that the model has the capability to describe some of the softening behavior seen in the experiment (Figure 6). Unfortunately, this trend has a limit, because for strains 1.8 and higher, the simulation experiences negative volume element errors, imposing a failure criterion dependent on mesh instability.

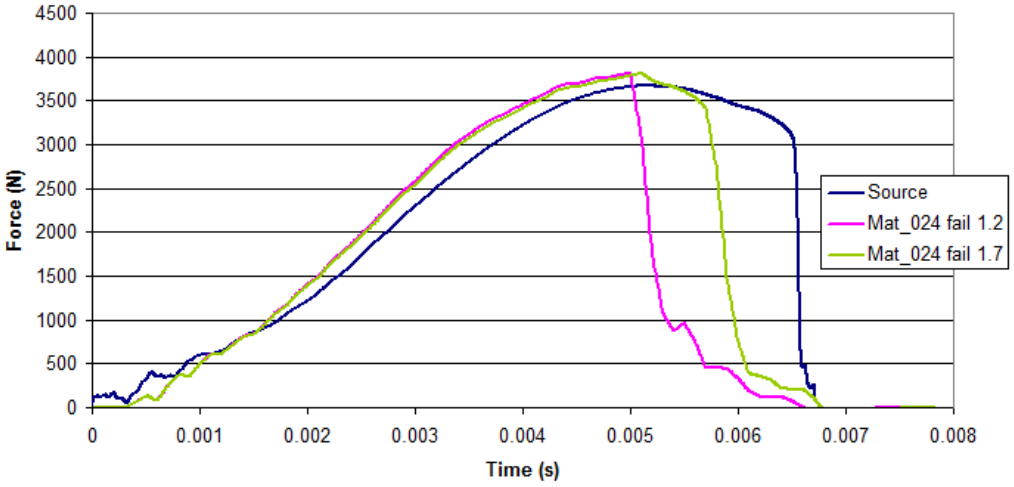

Figure 6: Effect of an increase in failure strain from 1.2 to 1.7 for ABS using MAT_024.

Simulation with MAT_089

For MAT_089, the yield stress is determined using an internal calculation based on the slope of the given true stress-strain curves. When the slope falls below the modulus specified by the user, the simulation assumes the material has yielded [4]. For rate dependency, the LCSR and Cowper-Symonds (CP) options seem to use the same formulation as in MAT_024. For the validation with MAT_089, the same quasi-static curve, now expressed as a true stress-strain curve, and the same values for rate-dependency used in the original MAT_024 simulations were used. It was noted that CP overpredicts while LCSR greatly underpredicts the experiment.

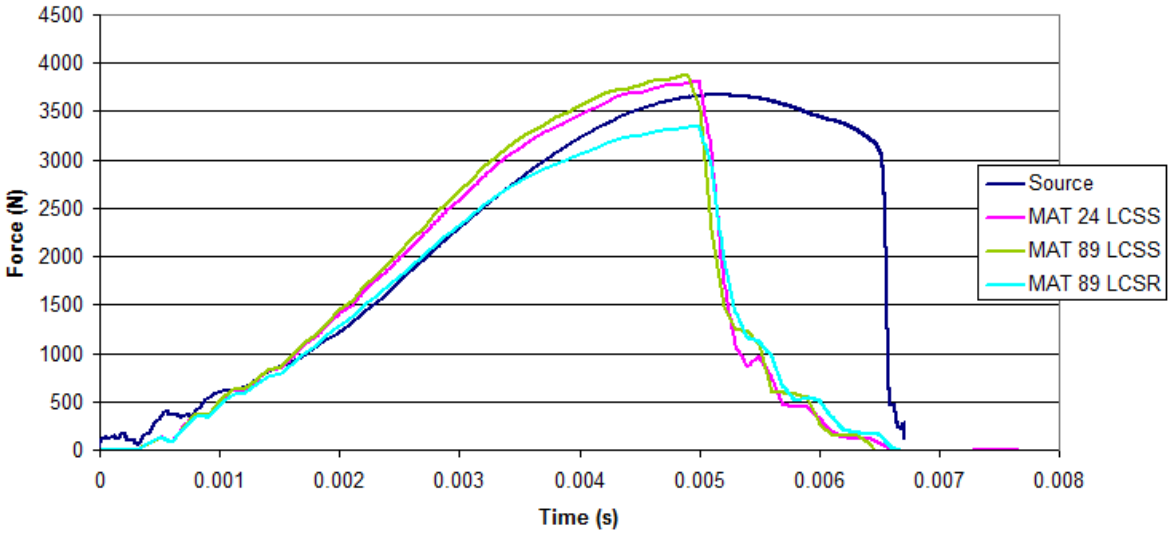

Figure 7: Comparison of MAT_089 LCSS and LCSR to MAT_024 LCSS.

This observation appears to correlate with others [6]. Using LCSS for MAT_089 seems to give the best case for ABS. The resulting curve is almost coincident with the MAT_024 curve. Again, increasing the failure strains improves the fidelity of the simulation up to a limit (Figure 8). For a failure strain of 1.8, negative volumes in elements trigger their deletion from the model.

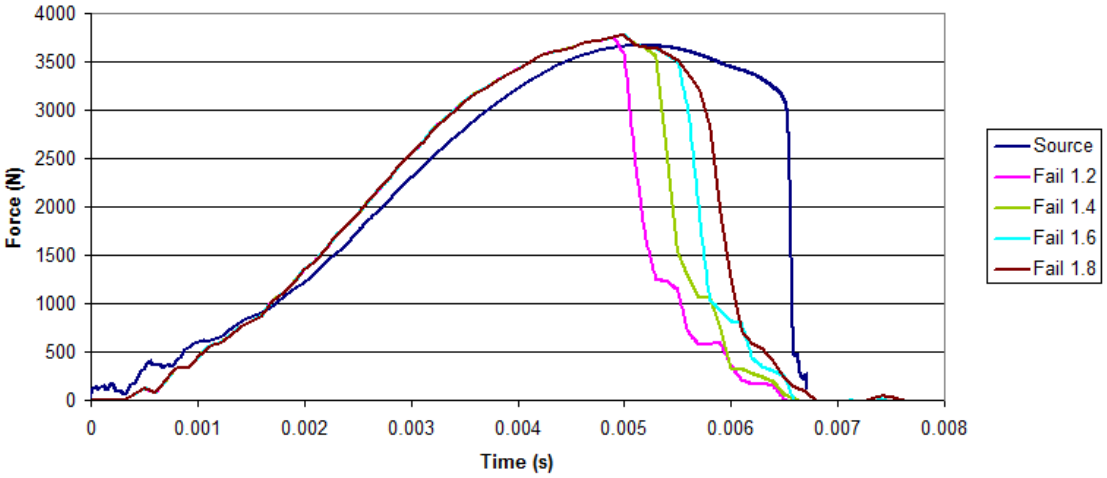

Figure 8: MAT_089 using LCSS settings with different failure strains.

In an attempt to understand why it was necessary to extend the failure strain beyond the measured tensile value, we examined the stress triaxiality ($-p/\sigma_{vm}$) of the bottom of the disk. It was noted that the failure occurred in a biaxial mode (Figure 9).

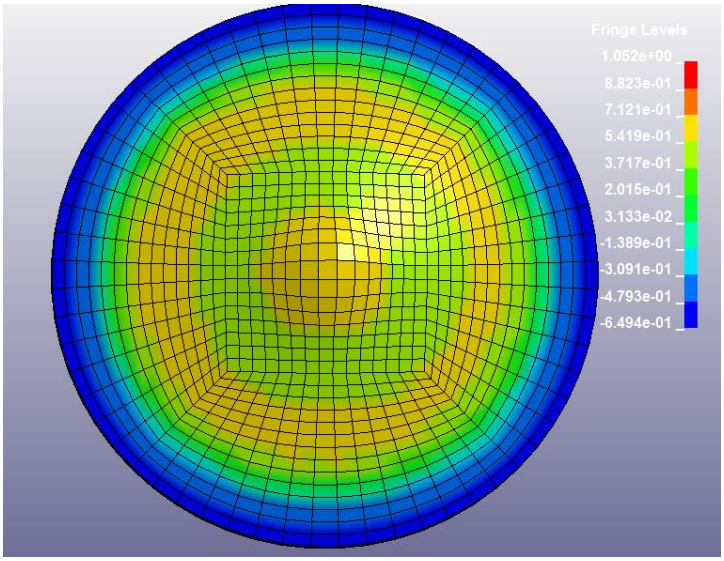

Figure 9: Triaxiality of the bottom of the disk before failure.

Using an Erichsen testing machine, we measured the biaxial failure strain of the ABS at quasi-static speed to be about 1.8 mm/mm. We also made a localized measurement of the quasi-static tensile (uniaxial) failure strain with DIC methods, yielding a value of 0.8 mm/mm. These findings suggest that the triaxiality dependence of failure strain could be a factor in failure

predictions with plastics, a feature that is not available in MAT_024 or MAT_089. For ABS, the failure strain in the tensile mode is unaffected by strain rate, so there was no opportunity to explore the effectiveness of the LCFAIL option of the MAT_089 model, which allows the modeling of failure strain as a function of strain rate.

The polypropylene has a failure strain that is highly dependent on the strain rate, as seen in (Figure 4). A MAT_089 model was created to probe if it was more capable of handling this behavior. The material properties used in the model were the same as in the previous work [1]. As with the ABS, we first attempted to discover whether arbitrarily increasing the failure strain beyond the originally used 1.2 value would yield a better result. In Figure 10, which shows the MAT_089 model with a larger failure strain of 1.6, we noted an improvement in the ability of the model to capture the failure point. As with the ABS, the LCSR formulation gave lower reaction forces than the test, while the LCSS option followed the experimental data quite well. However, a curious softening behavior was obtained during the initial stages of the simulation that was unique to the polypropylene.

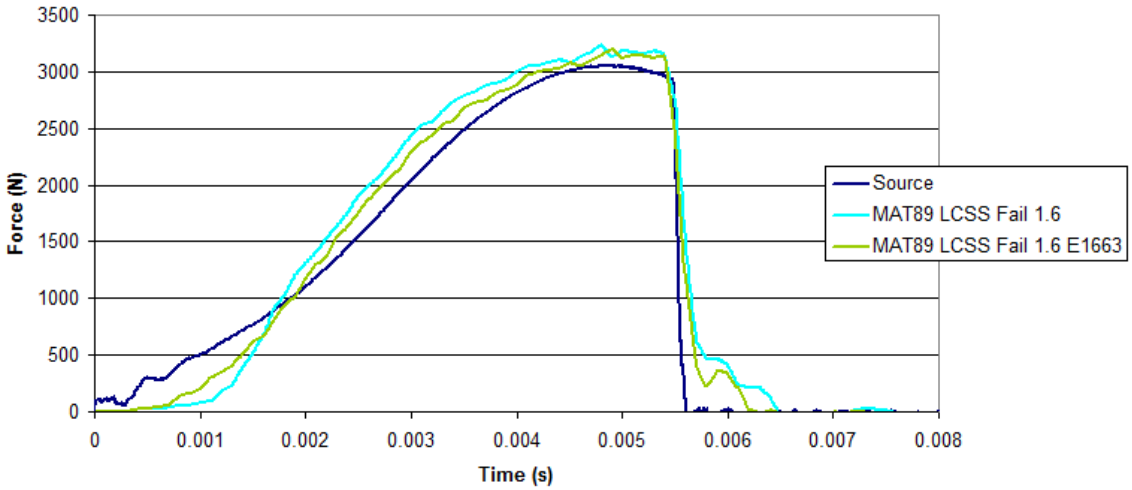

Figure 10: MAT_089 for polypropylene using LCSS settings with the highest and lowest elastic modulus values.

Probing this difference further, we noted that the polypropylene exhibits rate dependency of elastic modulus, while the ABS does not. Typically, for MAT_024 models, the highest modulus is used of the different stress-strain curves input to the model. Otherwise spurious energy generated might lead to an unstable simulation [4]. The MAT_089 formulation is somewhat better to model rate dependent modulus, depending on the choice of elastic modulus submitted to the model. The model allows for the input of higher strain-rate stress-strain curves with slopes steeper than the declared modulus; the simulation then internally increases the given modulus depending on the strain rate [4]. In the case of the ABS, since the material is not rate dependent in modulus, the simulation produces a result similar to MAT_024. With the polypropylene, when the highest modulus is used, the model declares the yield stress too early at the lower strain rates; the initial softening could be caused by the plasticity formulation calculating the stiffness differently than when only elastic strains are used. When the elastic modulus was changed to the lowest modulus corresponding to the slowest strain rate, a stiffer initial response was observed,

but not as good as that seen with the MAT_024 model. We can conclude that MAT_089 may have some issues simulating materials with rate-dependent modulus.

SAMP/MAT_187

In hopes of getting better correlation for the ABS, we moved on to MAT_187. For the initial pass, the model included a table of tensile curves at different strain rates, compressive stress-strain data and shear data with a plastic Poisson's ratio set to 0.5, mimicking the behavior of the MAT_024 and MAT_089 models. Failure strains were left at the default (1E+05). Biaxial data was not used.

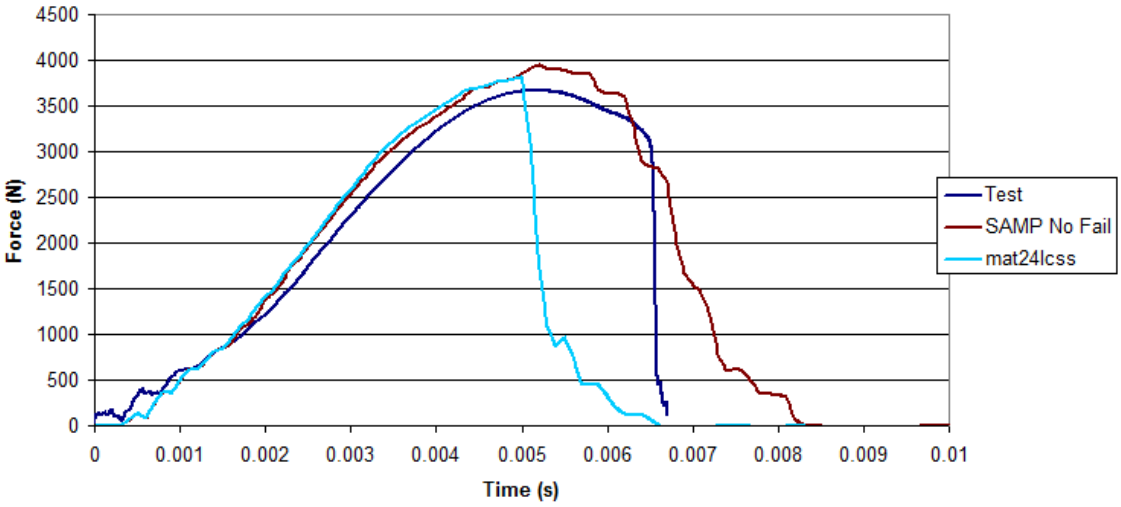

FigFig

Figure 11: MAT_187 for ABS using tension, compression, and shear stress-strain curves.

The resulting simulation produced a visibly acceptable result, including the ability to describe the softening behavior seen in the ABS, as seen in FigFigFigure 11.

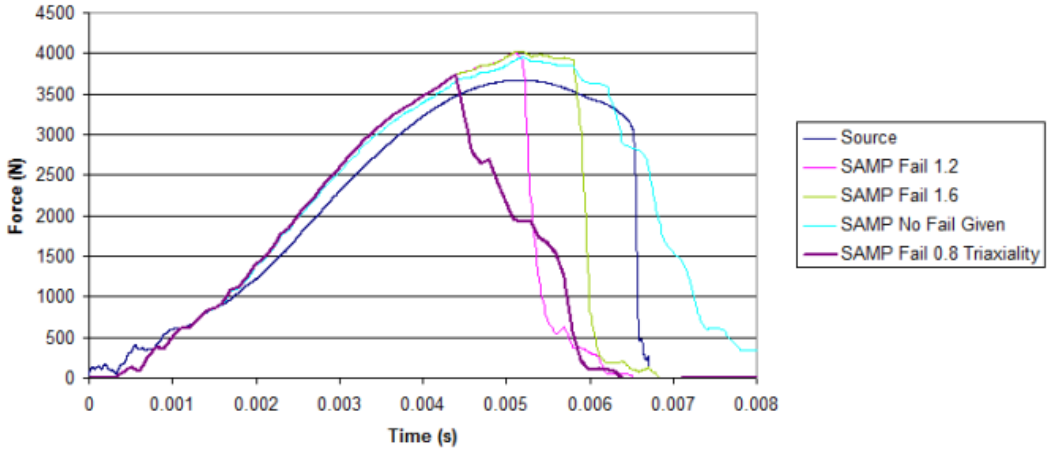

Figure 12: Effect of EPFAIL on simulation; applying measured failure strains using the triaxiality v. failure strain function.

However, using the default failure strain of 1E+05 led to negative volume errors, failure strains being determined by the geometry as opposed to an imposed value. Imposing failure strains in the vicinity of that obtained from the biaxial experiment and also used for other models resulted in similar "cut-off" behavior, with the additional benefit however, that the softening behavior was better captured by MAT_187 than the other models (Figure 12).We also attempted to use the EPFAIL and LCID-TRI failure options of MAT_187 to reconcile the difference in failure strain with triaxiality that was seen in the measured property data. Here, using a fail strain of 0.8 from the tensile measurement and 1.8 from the biaxial measurement, the simulation produced a premature failure as shown in Figure 12. We did not attempt to check whether reducing the mesh size would produce a better result

We turned to the effects of post-yield or plastic Poisson's ratio from there. Figure 13 plots Poisson's ratio against plastic strain, comparing the measured total Poisson's ratio to that calculated for plasticity by subtracting the elastic Poisson's ratio. We did not observe a significant difference between total measured post-yield Poisson's ratio and the computed plastic Poisson's ratio.

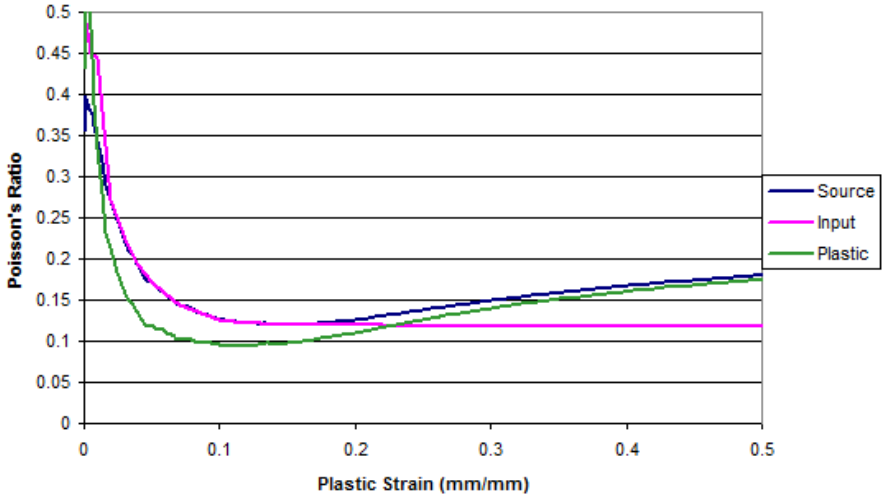

Figure 13: Mat_187 Poisson's ratio vs. plastic strain for ABS.

To invoke this option in MAT_187, the stress-strain data was recomputed to account for the post-yield Poisson's ratio using the following equation:

$$\sigma_t = \sigma_e(1+\varepsilon_e)^{2\nu p} \qquad (1)$$

where σ, ε, and νp are stress, strain, and plastic Poisson's ratio, and the suffices *e* and *t* refer to engineering and true notations. This equation replaces the constant of 0.5 used for the post-yield Poisson's ratio with the measured value instead. The effect of this change in calculation is observed in Figure 14. For contrast, the stress-strain curves to the left are based on the assumption that the plastic Poisson's ratio is 0.5 past tensile yield. It is also clear that Equation 1 reverts to the classical equation for the case of plastic Poisson's ratio of 0.5 used in the work up to now. The resulting curves used for the model are also overlaid in the figure.

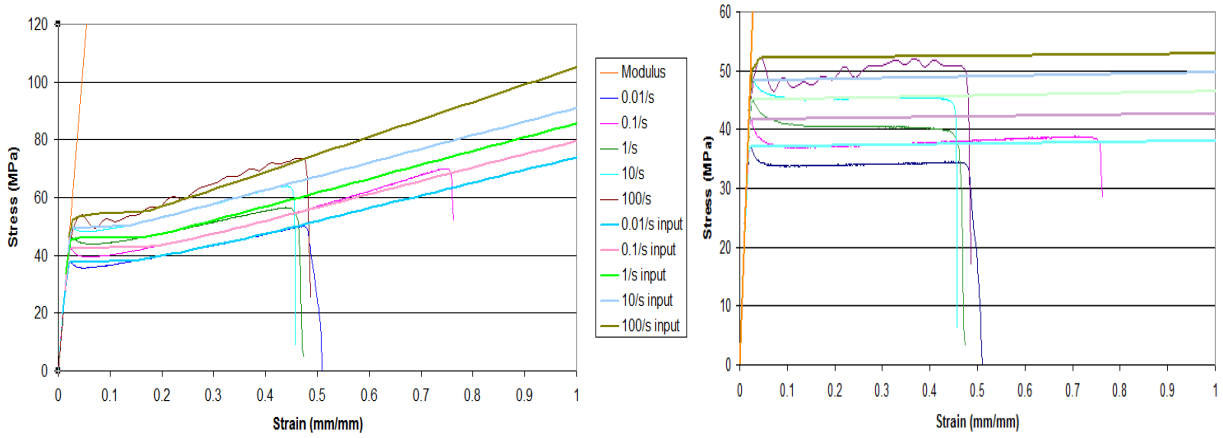

Figure 14: Test and extrapolated curves using the classical stress-strain calculation (left) and measured plastic Poisson's ratio (right).

The use of the plastic Poisson's ratio curve gave a softer response than with a constant 0.5 plastic Poisson's ratio as shown in Figure 15. Utilizing the same EPFAIL value of 1.6, the material failed at the correct time and displacement, performing better in this regard.

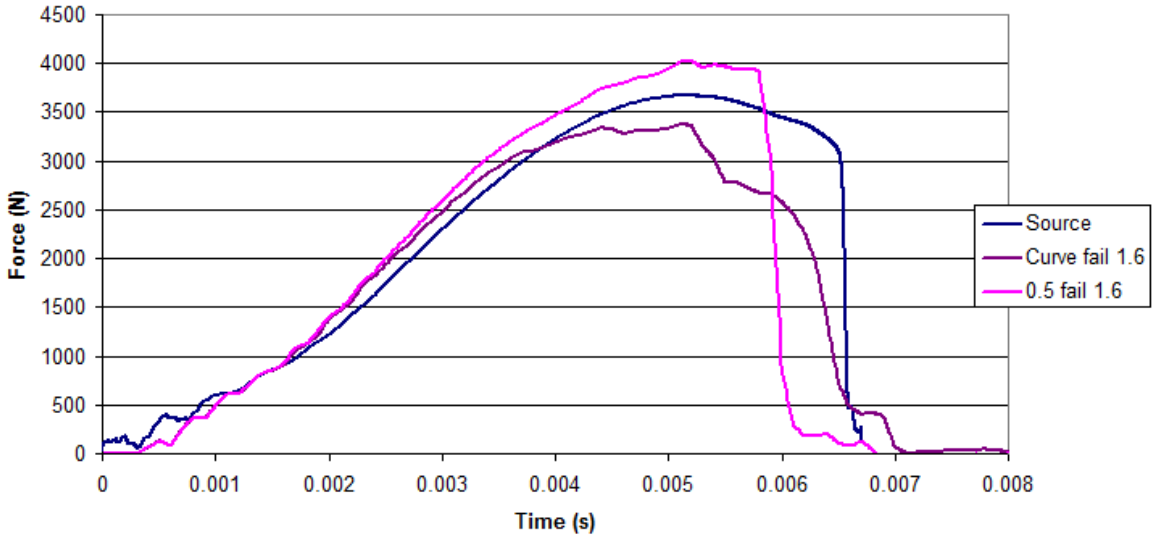

Figure 15: Mat_187 for ABS with measured plasticity Poisson's ratio and EPFAIL of 1.6.

Conclusions

Three LS-DYNA material models were validated against a standardized dart impact test. Validations were performed for two ductile plastics, an ABS and a polypropylene. While the ABS exhibited no rate dependency of failure strain, the polypropylene showed rate dependency in both modulus and failure strain. It was not possible to simulate the failure properly without extrapolation of the model beyond the measured failure strain in tension. One possible explanation may lie in the inability of the experiment to capture the extreme local deformation prior to failure[6]. By picking an arbitrary failure strain, however, it was possible to obtain a fairly good correlation for both materials. In an effort to understand why this extrapolation was

needed, experimental measurements showed that the biaxial strain at failure was indeed close to what was used in the simulation.

All three material models performed quite well in correlation. The MAT_024 material model performance was improved compared to the previous work by more careful extrapolation of the failure strain. Using that as a benchmark, we noted that MAT_089 performed as well in cases where the modulus is not rate-dependent. Only MAT_187 showed the capability to model the softening behavior prior to failure. The best correlation to experiment for the ABS was with the use of MAT_187 with the default failure strain of 1E05. However, the appearance of negative volume in elements made this an unacceptable outcome. In our use of MAT_187, we did not attempt to model unloading behavior using the technique proposed by Nutini [7] of using a damage model based upon the measured volumetric strain, but note that the damage curve can be easily calculated from our measured data.

It should be noted that the somewhat arbitrary choice of failure strain seems to be unavoidable with our approach. Considering that in this particular validation, the failure was biaxial in nature, it was possible to show the correlation by an actual measurement. However, it is unclear how universal this failure strain might be should failure in real-life components occur in shear or tensile modes. The rate-dependency of failure strain available in the MAT_089 model did not yield a positive result if we used the measured tensile fail strain values. Similarly, the use of the fail strain v. triaxiality function in the MAT_187 model did not provide a positive benefit. It is possible that experimentally, the material fails earlier in tension than it should because the triaxial state has changed prior to failure.

We also demonstrate the value of validation to test the simulation. The presence of a solid, reproducible benchmark of this kind is extremely valuable to test the various options of a material model and other simulation settings prior to use in real life applications.

Acknowledgements

We would like to thank Dr. Paul Du Bois, Dr. Morteza Kiani of ETA and Dr. Massimo Nutini of Lyondell Basell for their comments and assistance.

References

1. M. Lobdell, B. Croop and H. Lobo, “Comparison of Crash Models for Ductile Plastics,” 10th European LS-DYNA Conference. 2015.
2. H. Lobo, “Methodology for Selection of Material Models for Plastics Impact Simulation,” International LS-DYNA Conference. 2006.
3. H. Lobo, B. Croop and D. Roy. “Applying Digital Image Correlation Methods to SAMP-1 Characterization”, 9th European LS-DYNA Users' Conference. 2013.
4. “LS-DYNA Keyword User’s Manual: Volume 2 Material Models“, Revision:5442, , 154-160, 2014
5. S. Kolling, A. Haufe, M. Feucht and P.A.Du Bois, “A Constitutive Formulation for Polymers Subjected to High Strain Rates” 9th International LS-DYNA Conference. 2006.
6. M. Nutini, private communication (2016)
7. M. Nutini and M. Vitali, “Characterization of Polyolefins for Design Under Impact: from True Stress/Local Strain Measurements to the F.E.Simulation with LS-DYNA Mat. SAMP-1” LS-DYNA Anwenderforum, Bamberg. 2008.